23

Study of optical and cooperative parameters of fibrous quartz heat shielding on experimental data on its reflection spectra

© V.V. Cherepanov[1], R.A. Mironov[2]

[1] National Research University MAI,
125993 Moscow, Russia
[2] JSC ?ORPE ?Technologiya? named after A.G. Romashin,
249031 Obninsk, Russia

e-mail: vvcherepanov@yandex.ru

Received November 15, 2021
Revised November 15, 2021
Accepted April 6, 2022

The paper presents the results of a study of a number of key optical characteristics of some highly porous thermal protection materials based on amorphous SiO_2 fibers in the near and mid IR ranges. In the optical part of the statistical simulation model of such materials, based on the rigorous Mie theory, its application requires the introduction of cooperative corrections to the results of interaction with electromagnetic radiation of individual fragments. These corrections are introduced into the model in the form of an additional multiplier (C_s) of the scattering and absorption Mie efficiencies, which was usually used as a model tuning parameter when interpreting the experimental results of thermophysical studies. In this work, using the example of TZM-23M materials (Russia), made of a relatively thick $(\sim 9\,\mu\text{m})$ silica fiber PS-23 (Belarus), for the first time, data were obtained that make it possible to study the C_s parameter as a spectral quantity. The study is based on the results of experimental determination of the spectral hemispherical reflectivity of layers of material of two or more optical thicknesses in the wavelength range $0.83-16.65\,\mu\text{m}$. These data and Zege's asymptotic formulas were used to estimate the values of the absorption and scattering coefficients. The spectral parameter Cs is determined from the value of the scattering coefficient in the process of solving the inverse optical problem. The data obtained are compared with the results calculated on the basis of classical approximations of the optical constants. The results of this work can be useful for specialists in the field of radiation heat transfer and the interaction of electromagnetic radiation with complex partially transparent media with high spectral albedo scattering values.

Keywords: Silica fibrous thermal protection, reflectivity, experiment, absorption and scattering spectrum, optical model, Mie theory, cooperative corrections.

DOI: 10.21883/EOS.2022.07.54730.2930-21

Introduction

Thermally resistant fibrous materials are routinely used for thermal protection of internal units and structural elements in the aerospace industry. Their composition, porosity, anisotropy, flexural properties, and other mechanical characteristics vary within fairly wide ranges. Owing to the specifics of industrial applications, materials with high porosities up to 90% are of principal interest. Their thermal resistance varies within the $1.2-1.8\cdot 10^3{}^\circ\text{C}$ range, which defines the spectral region of importance for thermal transfer, since radiation in these materials is fairly close in its composition to equilibrium one. The radiation maximum corresponds to near-limit temperatures and wavelengths on the order of $1-3\,\mu\text{m}$. The typical average diameters of fibers are also close to this range. In Russia, TZMK [1] silica fiber materials produced by ORPE Technologiya in Obninsk (TZMK-10 (99.8% SiO_2) and TZMK-10M (99% SiO_2)) are commonly used. The degree of purity of amorphous quartz in them has a significant effect on both the spectral absorption coefficient and the cost of material production. The possibility of application of relatively cheap TZM-23M silica fiber (98% SiO_2) materials, which may be useful in certain contexts, is also being considered at present. The thickness of fibers in them $(\sim 9\,\mu\text{m})$ is significantly higher than the corresponding thickness in TZMK $(\sim 1.7\,\mu\text{m})$. Novel Russian VTI composites based on mullite-corundum fiber VVD-82, which were developed at the All-Russian Scientific Research Institute of Aviation Materials (Moscow), also hold promise for wide application due to their flexibility, enhanced thermal resistance, and gradient properties [2,3].

Owing to their high open porosity and the specifics of fragment-forming substances, such materials are partially transparent to electromagnetic radiation. Therefore, the thermal transfer in these systems at relatively high temperatures is primarily radiative in nature. However, such materials are often anisotropic and feature a high spectral scattering albedo. As a result, they entrap radiation at chaotically oriented framework elements and do not allow for any substantial heating of fragments of the base material due to a low absorption. The former factor limits the effective depth of radiation penetration into a material and the radiative heat flux, while the latter factor limits the thermal conductivity

over the framework. The heat-protective properties of materials are an immediate corollary of these limitations.

The significant influence of microscopic physical processes occurring in fibrous materials and their anisotropy, spatial inhomogeneity, and irregularity complicate considerably the calculation of physical characteristics and the characterization of radiation transfer and heat exchange in them based on heuristic continual approximations. However, since such materials are locally regular, one may introduce representative elements (REs) of a material and characterize their optical properties and other physical parameters [4,5]. Averaged characteristics of RE systems are interpreted in this approach as the properties of a material as a whole [6,7].

Although REs of fibrous materials are often formed from cylindrical elements, it is impossible to solve the problem of interaction of an RE with radiation within the rigorous electromagnetic theory. Therefore, the Mie theory solutions for individual long cylinders [8], which are then used to form solutions for an RE material, may serve as a basis for characterization. Naturally, since the use of a theory of interaction of individual bodies with the electromagnetic field may introduce substantial errors into the simulation results, the Mie theory should be applied with a certain correction. As was demonstrated in [9], a convenient way to perform such a correction is to introduce additional factor C_s into the efficiencies of Mie scattering and absorption of radiation by material fragments. It was also found that, in certain cases, this quantity allows for interpretation of the cooperative multilayering parameter in collective interaction of material fibers with electromagnetic waves. At $C_s < 1$, mutual screening of fibers, which reduces their effective cross sections, is probable, while $C_s > 1$ suggests that an individual fiber distorts an incident wave only weakly, and the process of wave–material interaction involves fibers located in subsequent layers lying in the direction of wave propagation. As a free parameter of the optical part of the simulation model, C_s provides an opportunity to adjust it to the available experimental data, interpret the experiment, and calculate a number of additional material characteristics that are practically impossible to determine without specialized (and often costly) equipment.

Unfortunately, data on the spectral properties of high-porosity thermal insulation have until recently remained largely fragmentary. For example, the authors of [10] determined optical parameters using an analytical-experimental method in the diffusion approximation. Measurements were performed with cylindrical samples and probing laser radiation at just three wavelengths (0.63, 1.15, and $3.39\,\mu$m). The diffusion approximation was also used in [11] to measure the transmission coefficients for samples of various thickness in a rather limited wavelength range ($0.4-0.75\,\mu$m). Therefore, the results of a thermophysical experiment have normally been used to adjust C_s in actual simulations, and this quantity was defined as a function of thermodynamic parameters. This factor prevented one from considering and analyzing parameter C_s as a spectral characteristic of a material (which is definitely true of C_s [9,12]).

The aim of the present study is to fill this gap. The study is based on the results of experimental determination of the spectral hemispheric reflectance of layers of a fibrous material of two or more optical thicknesses for a considerable number of wavelengths (up to 7520) from the $0.83-16.65\,\mu$m range. These data and the known analytical solutions of the inverse optical problem [13–15] are used to calculate the absorption and scattering coefficients of the spectral kinetic equation of radiation transfer. Notably, TZM materials differ from TZMK in that the problem of determination of these optical characteristics was of interest on its own, since they have never before been subjected to such examination. Owing to the relative weakness of absorption, spectral parameter C_s is determined numerically based on the scattering coefficient in the process of solving another inverse optical problem. The obtained data are compared to the figures calculated using classical approximations of optical constants.

1. Experimental data and calculation procedure

Disk-shaped samples of materials with a diameter of 30 mm and a thickness of $1-20$ mm were prepared for the study of spectral optical properties of fibrous thermal insulation. Measurements were performed using a Nicolet is50 Fourier spectrometer with an IntegratIR (PIKE) integrating sphere with an aperture of 30 mm and a spot diameter of ~ 3 mm under normal radiation incidence. The obtained values were referenced to a gold reflection standard. Since the considered fibrous materials are fairly hygroscopic, the samples were dried at a temperature of 120°C for 3 h prior to measurements.

In measurements on an integrating sphere, the samples have a simple geometry and the size of the incident radiation beam is much smaller than the sample diameter; therefore, the samples may be considered to be infinite in the lateral direction. A plane-parallel model of a sample with thickness h, which was also considered to be optically uniform and immersed into a non-absorbing medium with a unit refraction index, was thus used to process the experimental data.

According to [13], an asymptotic regime is established in an optically thick scattering and absorbing layer. This regime is characterized by the separation of angular and spatial variables, azimuthal field independence, and exponential decay of the intensity with depth. This factor makes it considerably simpler to solve inverse problems of identification of optical material properties. Fairly accurate values of absorption and scattering coefficients of a unit material volume may be obtained by measuring (under directional illumination) either hemispheric coefficients of total reflection and transmission of a material layer, which are hereinafter referred to as reflection and transmission

coefficients, or the reflection coefficients of samples of two (or more) different thicknesses. The relationship between these quantities, which is known as asymptotic formulae, comes down to simple analytical relations of the following form [14,15]:

$$R(\tau,\mu_0)=\frac{\mathrm{sh}(X)}{\mathrm{sh}(X+Y)},\qquad T(\tau,\mu_0)=\frac{\mathrm{sh}(Y)}{\mathrm{sh}(X+Y)},$$

$$R_\infty=e^{-Y},\qquad X=\Gamma\tau-4q\Gamma\varphi(\mu_0),$$

$$Y=4q\Gamma\varphi\mu_0),$$

$$\Gamma=1-\Lambda\sqrt{3-x_1}[\Lambda(1-\Lambda)]^{(1+\Lambda^4)^{-1}},\qquad(1)$$

$$\Lambda=\beta/\varepsilon,\quad \tau=\varepsilon h=(\alpha+\beta)h,$$

$$q=(3-x)^{-1},\qquad \varphi(\mu_0)=3(1+2\mu_0)/7.$$

Here, R, T are the reflection and transmission coefficients of a layer with optical thickness τ, Λ is the spectral scattering albedo, φ introduces a correction for illumination conditions (μ_0 is the cosine of the angle of incidence onto a layer), x_1 is the first coefficient in the expansion of the scattering indicatrix in Legendre polynomials, and index ∞ denotes the quantities corresponding to a semi-infinite layer. Thus, the reflection and transmission functions of layers of a significant optical thickness are expressed in terms of the reflection parameters of a semi-infinite layer. Relations (1) are formulated with account for the fact that the reflection off sample–air interfaces may be neglected in the case of radiation incidence from the bulk of the considered high-porosity materials.

It was demonstrated in [16] that the region within which these relations are satisfied accurately to within the $O(\Gamma^2)$ terms, where $\Gamma<1$, is bounded by conditions

$$Y\le 1,\qquad \tau\ge 4q.\qquad(2)$$

However, the examination of this issue in [17] revealed that the error of asymptotic formulae in calculation of the scattering coefficient for quartz ceramics does not exceed several percent outside of boundaries (2) (even outside of the transparency region).

This is quite sufficient for the purposes of the present study. To achieve its objectives, we first determine the values of X and Y using the first relations in (1), the $R(\tau_{1,2},\mu_0)$ values for samples of two finite optical thicknesses, or the values of $R(\tau,\mu_0)$ and $R_\infty(\mu_0)$. The remaining equations allow one to determine attenuation ε and scattering albedo Λ, which are then used to calculate α and β.

Since the absorption coefficient corresponding to the considered materials and spectral region is normally 2–3 orders of magnitude lower than the scattering coefficient, spectral β values were used to identify parameter C_s. Simulation statistical modeling of the spectral material properties is performed repeatedly for each of the considered wavelengths to find a value of C_s that provides the needed β. The procedure of statistical modeling of fibrous materials has been characterized thoroughly in [5,7,9]. Since the algorithm for searching for C_s in not crucial to the present study, it is not detailed here.

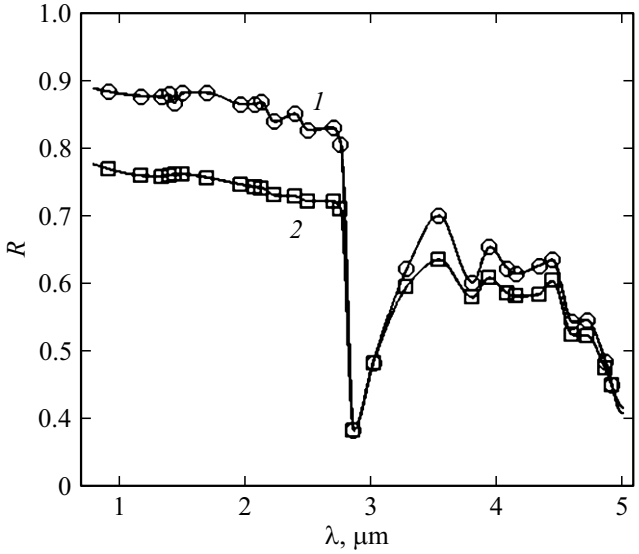

Figure 1. Spectral coefficients of total reflection R for two TZMK-10M samples with a thickness of 1.07 (*1*) and 12.51 mm (*2*).

We note in conclusion that the software tools at our disposal are proprietary and provide an opportunity to calculate one spectral point with statistics up to 10^4 REs (in most cases, the sought-for spectral characteristics of an RE system are identified accurately with smaller statistics) within 1–1.5 min on a computer with an Intel Core I7 processor with a clock frequency of 3.3 GHz. Although one C_s value was commonly identified in no more than ten steps with statistical simulation, the overall identification time remained prohibitively long, since the experimental data set contained more than 7000 spectral points with reflection coefficients for wavelengths from the 0.83–16.7 μm range. To reduce the amount of calculation, only the points of spectral extrema of α and β were included into the process of C_s identification. This allowed us both to factor in the key features of absorption and scattering spectra and to reduce the overall amount of calculation by a factor of approximately 7.

2. Results and discussion

Figure 1 presents the spectra of reflection coefficients for two samples of TZMK-10M with a density of 139 kg/m^3 and different thickness (1.07 and 12.51 mm) in the high-transparency region of high-purity amorphous quartz. The reflection coefficient corresponding to the sample with the larger geometric thickness remains higher throughout almost the entire studied wavelength range. Intense reflection and a distinct „plateau“ of the reflection coefficient are observed at relatively short wavelengths. Owing to intense absorption, the samples have almost equal reflection coefficients in the

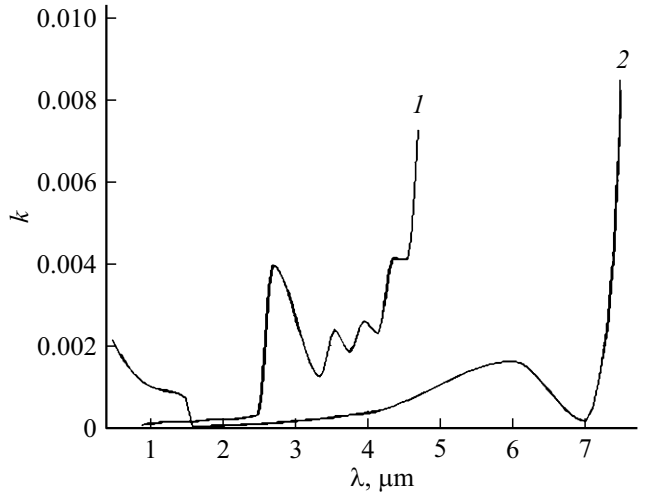

Figure 2. Absorption indices of TZMK-14M (TKV quartz fiber, Russia) and high-purity amorphous quartz [18-20].

region of absorption of hydroxyl groups ($2.5-3\,\mu$m). The transparency of TZMK-10M in the near IR range turned out to be lower than the one of TZMK-10, which was once used in thermal protection of the Buran frame. Absorption index k of TKV quartz fiber (Russia), which is the material used to fabricate TZMK-10M, starts increasing rapidly already at $4\,\mu$m, while the absorption index of high-purity amorphous SiO_2 increases only at $\sim 7\,\mu$m [18–20] (Fig. 2).

The results presented in this figure were obtained in the process of adjusting the absorption index of the material to the spectral values of absorption coefficient α calculated using the data from Fig. 1 and relations (1). Since the layer with a thickness of 12.51 mm had almost zero transmission in the spectral region shown in Fig. 2, the data for this layer were interpreted as R_∞ in the processing of experimental results.

Similar data of R measurements in the frequency region corresponding to a wavelength range of $0.83-16.65\,\mu$m for TZM-23M materials with a density of 142 and 392 kg/m^3 are presented in Fig. 3. Samples with a thickness of ~ 20 mm were used in experiments. The reflection spectrum of these samples behaves in a similar fashion to the one in Fig. 1 in the region of absorption of hydroxyl groups; in common with TZMK materials, it also features a reflection plateau.

It may seem that the presence of a plateau in the reflection spectra of TZMK and TZM does not fit the behavior of R in the classical model of optical constants [8], which comes down to the following relations in the single-oscillator version:

$$\varepsilon = \varepsilon_1 + \varepsilon_2 = n^2 - k^2 + 2nk = \varepsilon_0 + \frac{\omega_p^2}{\omega_0^2 - \omega^2 - i\gamma\omega},$$

$$R = \frac{1-\delta}{1+\delta},$$

$$\delta = \sqrt{2}\frac{\sqrt{\varepsilon_0 + 2\rho + p/f}}{1+2\rho}, \quad 2\rho = \sqrt{\left(\varepsilon_0 + \frac{p}{f}\right)^2 + \frac{q^2}{f^2}},$$

$$p = \omega_p^2\left(\omega_0^2 - \omega^2\right), \quad q = \gamma\omega\omega_p^2,$$

$$f = \left(\omega_0^2 - \omega^2\right)^2 + \gamma^2\omega^2. \qquad (3)$$

According to this model, the reflection coefficient should decrease in the high-frequency region as $O(\omega^{-4})$. Therefore, the presence of a high-frequency plateau in Figs. 1 and 3 should be interpreted as a consequence of destruction of the initial structure of materials in the near-surface region in the process of preparatory processing of samples. However, classical model (3) also allows for the presence of an R plateau of a finite width in the soft-wave region. This is demonstrated by curve R_c in Fig. 3, which corresponds to parameters $\varepsilon_0 = 1$ and $\omega_p = 2\cdot 10^{15}$, $\omega_0 = 1.1\cdot 10^{15}$, $\gamma = 10^{12}$ (Hz) of the classical model. It is worth reminding that ω_0, ω_p in (3) are the natural and plasma frequencies, and parameter γ characterizes dissipation effects. A plateau simply covers a part of the frequency range visible in the figure, and the value of R_c starts decreasing at the needed rate when the frequency increases further. Note that a similar behavior of reflection spectra was observed for quartz ceramic samples with a substantially lower porosity (down to 10%) in experiments where the preparatory surface treatment could not induce such radical structural damage and variation of properties [17].

However, in addition to experimental dependences, we considered approximations of the reflection coefficient by functions of the form

$$R(\omega) = \frac{a}{(\omega^2 - \omega_0^2)^2 + \gamma^2\omega^2}, \qquad (4)$$

which have a single maximum point and a „proper" behavior at the edges of the spectrum ($R(\omega) \sim O(\omega^{-4})$ at high frequencies and $R'(0) = 0$ at low frequencies) at

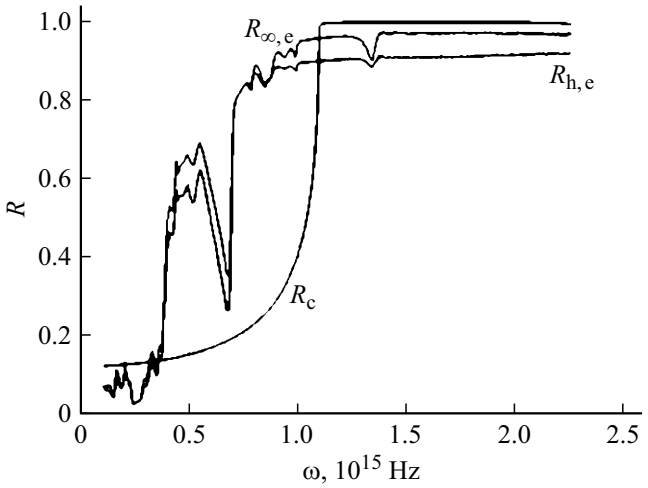

Figure 3. Spectrum of reflection coefficient R of TZM samples and data provided by the single-oscillator version of the classical model of optical constants [8] with adjusted parameters.

Parameters of functions (4) defining the $R_{\infty,\mathrm{m}}$ approximation in Fig. 4

№	R_0	R_m	$\omega_\mathrm{m} \cdot 10^{-14}$, rad/s
1	0.0213	0.60228	5.4961
2	0.00213	0.20076	4.9465
3	0.0184	0.449979	4.3969

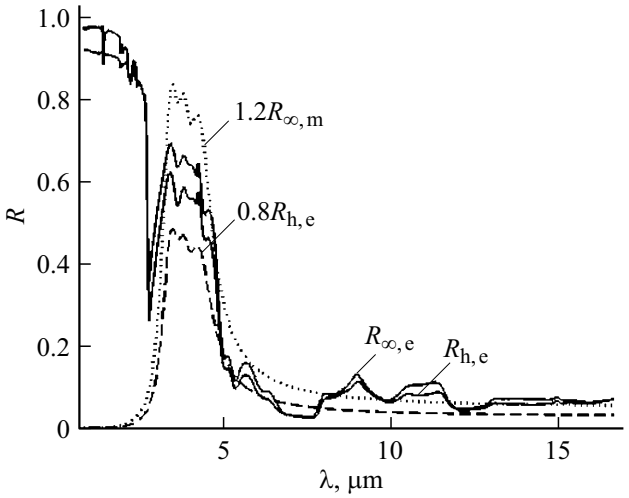

Figure 4. Spectral reflection coefficients R_h and R_∞ obtained (e) experimentally and (m) by summing three dependences (4) with specially adjusted parameters (see the table).

moderate γ values. Functions (4) do not feature plateau regions, but make it easy to plot approximations reproducing well-defined maxima in the experimental spectra of R. Apart from the values of a, ω_0, and γ, function (4) may be specified by the value of $R(0) = R_0$ corresponding to the low-frequency boundary and parameters R_m and ω_m of the maximum point, which are more convenient for choosing an approximation variant in simulation. These groups of parameters are bound by very simple relations

$$a = R_0\omega_0^4, \quad \gamma = \omega_0\sqrt{2\left(1-\sqrt{1-\frac{R_0}{R_\mathrm{m}}}\right)},$$

$$\omega_0 = \omega_\mathrm{m}\left(1-\frac{R_0}{r_\mathrm{m}}\right)^{-1/4}.$$

The parameters of three functions of the form (4) are listed in the table. A sum of these functions forms a simplified model of the reflection coefficient of a semi-infinite layer, $R_{\infty,\mathrm{m}}$; this model takes into account the specific features of behavior of the measured R spectrum in the $2.5-5\,\mu$m wavelength range and features moderate deviations from experimental curves at relatively long wavelengths. The approximations are represented by dashed curves with index „m“ in Fig. 4, while the experimental curves have index „e.“ $R_{\mathrm{h,m}} = 0.87R_{\infty,\mathrm{m}}$.

Figure 5 demonstrates the spectra of absorption $\alpha(m^{-1})$ and scattering $\beta(m^{-1})$ coefficients for TZM-23M with a density of 142 kg/m^3 calculated based on the experimental (a) and model (b) values of reflection coefficient R using asymptotic Zege relations (1). The spectra of parameter C_s, which were determined based on β values from the solution of the corresponding inverse problem, and piecewise-constant criterial function Crit, the lower value of which corresponds to region (2) of compliance with asymptotic formulae (1) with a high accuracy, are also shown in the same figure.

Since the reflection spectrum model based on the representation of a material layer as a dense system of oscillators yields a stronger absorption, conditions (2) are satisfied less tightly in it. The behavior of the scattering coefficient in the model is largely similar to the behavior of the reflection coefficient; therefore, scattering is the cause of the strongest reflection in this case. The effects of absorption in the region of strong scattering are weakened significantly in the model.

In the near IR range, the scattering coefficient of the real material first essentially follows the reflection coefficient (see Fig. 5, a) and assumes relatively high values, and then the index and the coefficient of absorption of hydroxyl groups start increasing rapidly. This immediately translates into an enhancement [8] of the effects of reflection off framework elements and leads to an almost resonant jump of the scattering coefficient. It will be shown below that real high-porosity materials are characterized by an irregular and resonant behavior of scattering, absorption, and extinction spectra. In contrast to the model spectra from Fig. 5, b, the absorption and scattering spectra of real materials have no correspondence between the minima of α and the maxima of β (and vice versa). It has already been noted that these factors are among the ones limiting the applicability of various continual models in detailed characterization of the optical properties of existing high-porosity materials.

The spectral behavior of C_s, which is presented in Fig. 6, is also of interest (especially in the region of weak absorption at short wavelengths $\lambda < 2.3\,\mu$m).

Monotonic dependences on temperature (and, consequently, on Wien wavelength [21]) are normally obtained for C_s when the model is adjusted to the data of thermophysical experiments. Similar (basically monotonic) C_s dependences have been proposed earlier in interpretation [9] of the results of the spectral experiment [10] with TZMK-10, where a local deviation from monotonicity of the C_s spectrum was associated with the specifics of the diameter distribution of fibers in this material.

Figure 6, b demonstrates a series of regularly positioned broad maxima and minima of C_s, which are present in equal measure in the „experimental“ (e) and model (m) curves. The model dependence has significantly weaker pulsations, since both scattering coefficient β and the corresponding C_s values in the short-wavelength range are reduced considerably due to the elimination of strong absorption in the short-wavelength region in the used R model. A certain correspondence between maxima and minima is seen in pulsations in both curves. The lack of association between this C_s behavior and calculation effects

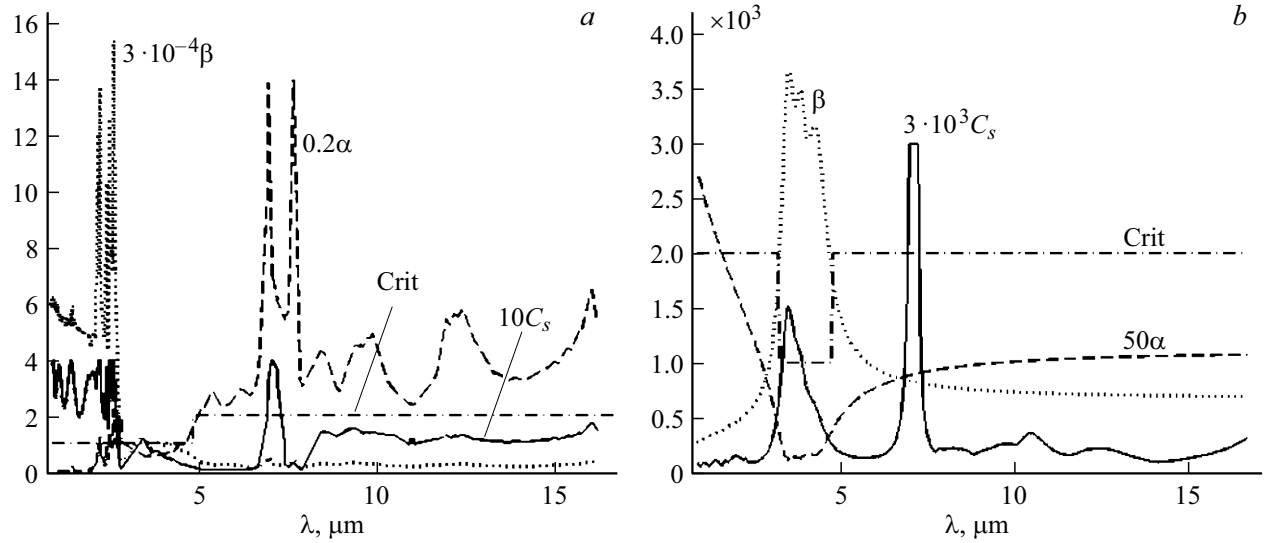

Figure 5. Spectra of absorption $\alpha(m^{-1})$ and scattering $\beta(m^{-1})$ coefficients, which were calculated based on the experimental (a) and model (b) values of reflection coefficient R, and the corresponding spectra of parameter C_s. The lower value of piecewise-constant function Crit denotes the region of satisfaction of conditions (2). The material is TZM-23M with a density of 142 kg/m^3.

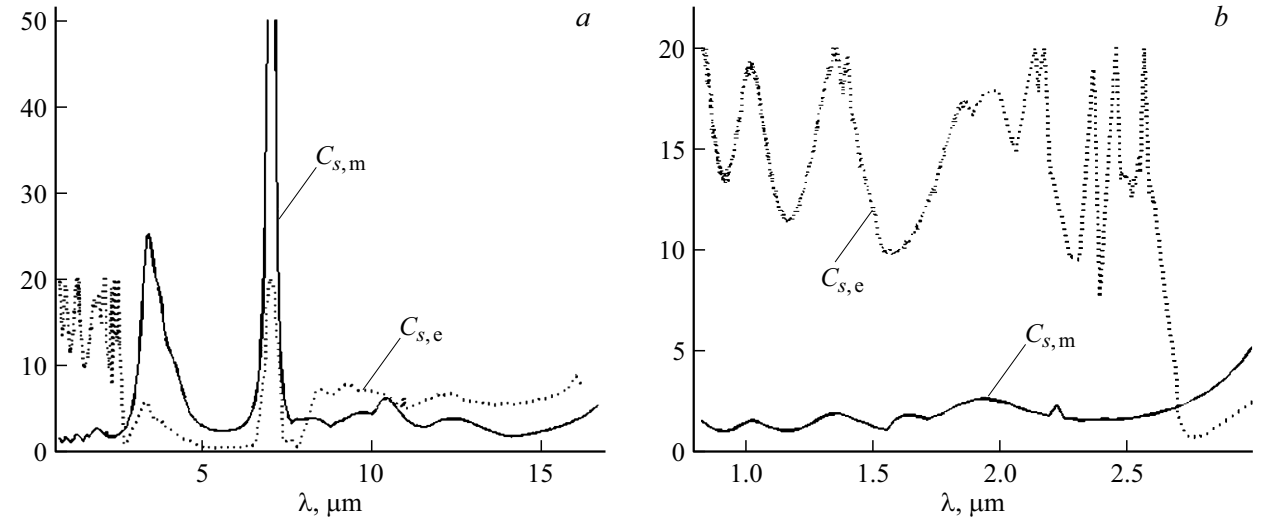

Figure 6. Experimental (e) and model (m) spectra of C_s (a) and the initial section of the spectrum with large-scale fluctuations (b).

is verified indirectly by the fact that the computational points on „experimental" and model curves differed. The wavelengths in experimental R spectra for which the α and β spectra were also calculated were not equidistant, and the number of equidistant points used to plot the model dependence was two times lower.

Note that oscillations of transmission and reflection coefficients of a uniform layer with a finite thickness have long been known [8]. A behavior closer to the one demonstrated in Fig. 6, b with regular and relatively large-scale pulsations (interference structure) and a superimposed fine structure in the form of small-scale irregular low-amplitude pulsations (ripple) was observed in the region of weak absorption in extinction spectra of systems of certain particles with a size on the order of a micrometer. These effects have also been examined in sufficient detail in [8] and are attributable to the specific features of coefficients of particle scattering series in the Mie theory. However, the present case is unusual in that the reflection, scattering, and extinction spectra of the considered fibrous system do not exhibit this behavior (i.e., the one typical of C_s). Therefore, the presence of the interference C_s structure cannot be attributed directly to the above causes. The only feature in common with the phenomena characterized in [8] is the fact that they are observed in the region of weak absorption of systems of particles with sizes on the order of a wavelength.

Both the model $C_s(\lambda)$ dependence and the curve plotted based on experimental data feature maxima in the vicinity

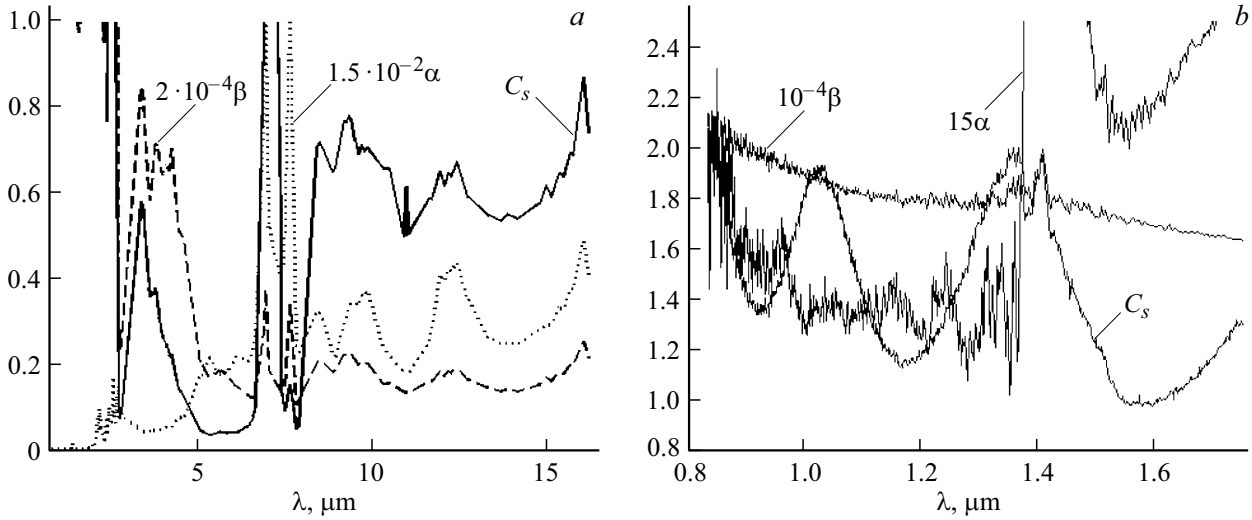

Figure 7. Comparison of the C_s spectrum with the spectra of absorption $\alpha(m^{-1})$ and scattering $\beta(m^{-1})$ coefficients within the entire studied wavelength range (a) and in its initial section (b).

of 3.5 and 7.1 μm. This is seen particularly clearly in Fig. 6, a, where the „experimental" and model spectra of parameter C_s are presented in the same scale. However, the C_s maxima of the model curve are significantly more prominent: a considerable portion of the peak in the vicinity of $\lambda \sim 7.1\,\mu$m had to be „cut" in order to fit it into the figure.

Figure 7 presents the spectra of α, β, and C_s in a scale that differs somewhat from the one in Fig. 5, a. The above-mentioned resonant nature of absorption and scattering spectra is evident in Fig. 7, b. Note also that the maxima in the vicinity of 3.5 and 7 μm are present simultaneously (see Fig. 7, a, the spectra of α, β, and C_s), but have different relative heights. Specifically, the peak near $\lambda \sim 7.1\,\mu$m and its closest „neighbor" at $\sim 7.6\,\mu$m are the most pronounced in the absorption spectrum and have a resonant nature there. They are much weaker in the β and C_s spectra, thus emphasizing the dominant influence of β on C_s. This is hardly surprising, since the cooperative parameter was determined based on the scattering coefficient. However, in contrast to C_s, the scattering coefficient reveals no large-scale fluctuations in the region of short waves and the reflection plateau in Fig. 7, b. The behavior of β is characterized almost exclusively by „ripple" fluctuations; its spectrum features no large-scale structures. Such structures are visible in the spectrum of the absorption coefficient in Fig. 7, b, where they are „masked" somewhat by resonance phenomena. However, they do not correspond to the behavior of C_s and cannot be used to interpret its large-scale features. Note also that the maxima points indicated above cannot be associated directly with any geometric parameters of fibers of the TZM-23M material (i.e., their diameters $d \in [8.4,\ 9.7]\,\mu$m, average diameter $\langle d \rangle = 9.05\,\mu$m, or characteristic length-to-diameter ratio $\langle l/d \rangle \sim 10$). In addition, all the quantities in Fig. 7, a behave in a similar fashion at wavelengths close to the diameters of material fibers (or exceeding them). However, comparing Figs. 7, a and 4, it is hard to argue that any of the quantities (α, β, C_s, and reflection coefficient R) behave similarly in this spectrum region.

This complex multiscale behavior of the parameters of fibrous thermal insulation makes it difficult both to characterize its optical properties and to interpret C_s as a spectral characteristic. Naturally, it requires further study, since parameters similar to C_s have virtually no alternatives in simulation modeling (owing to the evident limitations of analytical methods with a rigorous approach to the characterization of electromagnetic processes on the microlevel of heterogeneous systems).

Conclusion

Novel data on the spectral parameters of high-porosity fibrous thermal-protection materials produced in Russia from amorphous SiO_2 of various degrees of purity were obtained. The reflection, scattering, and absorption spectra of these materials were measured and analyzed for the first time in the near and middle IR range, and a specific characteristic of such materials, which may provide data on poorly studied cooperative processes occurring in the interaction of their fragments with electromagnetic radiation, was examined. A number of intriguing features of behavior of spectral properties of such systems were identified, and their interrelations, which cannot be investigated without a spectral experiment, were analyzed. Both known and well-proven experimental techniques and original efficient tools for theoretical examination, analysis, and prediction of material properties were used in the study.

Funding

This study was supported financially by the Russian Foundation for Basic Research (grant No. 20-08-00465).

Conflict of interest

The authors declare that they have no conflict of interest.

References

[1] A.G. Romashin, M.Yu. Rusin, F.Ya. Borodai. Refract. Ind. Ceram., **45** (6), 387 (2004).
[2] B.V. Shchetanov, Yu.A. Ivakhnenko, V.G. Babashov. Russ. J. Gen. Chem., **81** (5), 978 (2011).
[3] L.V. Gerashchenkov, Yu.A. Balinova, E.V. Tinyakova. Glass Ceram., **69** (3–4), 130 (2012).
[4] W.W. Sampson. *Modeling stochastic fibrous materials with mathematica* (Springer Nature, London, 2009). DOI:10.1007/978-1-84800-991-2
[5] V.V. Cherepanov, O.M. Alifanov. Comp. Appl. Math., **36**(1), 281(2017). DOI: 10.1007/s40314-015-0229-0
[6] J.-F. Sacadura. Heat Trans. Eng., **32**(9), 754(2011). DOI:10.1080/01457632.2011.525140
[7] V.V. Cherepanov, O.M. Alifanov. J. Heat Trans., **139**(3), 032701(2017). DOI:10.1115/1.4034814
[8] C.F. Bohren, D.R. Huffman. *Absorption and scattering of light by small particles* (Wiley, Ney York, 1983).
[9] O.M. Alifanov, V.V. Cherepanov. *Metody issledovaniya i prognozirovaniya svoistv vysokoporistykh teplozashchitnykh materialov* (MAI, Moscow, 2014) (in Russian).
[10] A.V. Kondratenko, S.S. Moiseev, V.A. Petrov, S.V. Stepanov. High Temp., **29** (1), 126 (1991).
[11] A.V. Zuev, P.V. Prosuntsov. J. Eng. Phys. Thermophys., **87**(6), 1374(2014). DOI:10.1007/s10891-014-1140-z.
[12] V.V. Cherepanov. Tepl. Protsessy Tekh., **9** (7), 448 (2017) (in Russian).
[13] S. Chandrasekhar. *Radiative transfer* (Oxford, London, 1950). DOI: 10.1002/qj.49707633016
[14] E.P. Zege, A.P. Ivanov, I.L. Katsev. *Perenos izobrazheniya v rasseivayushchei srede* (Nauka i Tekhnika, Minsk, 1985) (in Russian).
[15] A.P. Ivanov, V.A. Loiko, V.P. Dik. *Rasprostranenie sveta v plotnoupakovannykh dispersnykh sredakh* (Nauka i Tekhnika, Minsk, 1988) (in Russian).
[16] E.P. Zege, O.V. Bushmakova, I.L. Katsev, N.V. Konovalov. J. Appl. Spectrosc., **30** (5), 646 (1979).
[17] R.A. Mironov, M.O. Zabezhailov, M.Yu. Rusin, V.V. Cherepanov, S.P. Borodai. High Temp., **54** (5), 682 (2016). DOI: 10.7868/S0040364416040153 [R.A. Mironov, M.O. Zabezhailov, M.Yu. Rusin, V.V. Cherepanov, S.P. Borodai. High Temp., **54**(5), 682(2016). DOI: 10.1134/S0018151X16040143].
[18] R. Kitamura, L. Pilon, M. Jonasz. Appl. Optics, (33), 8118(2007). DOI:10.1364/AO.46.008118
[19] J. Kischkat, S. Peters, B. Gruska, M. Semtsiv, M. Chashnikova, M. Klinkmuller, O. Fedosenko, S. Mochulik, A. Aleksandrova, G. Monastyrsyi, Y. Florez, W.T. Masslenik. Appl. Optics, (51), 6789(2012). DOI:10.1364/AO.51.006789
[20] L.V. Rodriguez de Marcos, J.I. Larruquert, J.A. Mendez, J.A. Aznarez. Opt. Mat. Exp., (6), 3622(2016). DOI:10.1364/OME.6.003622
[21] V.V. Cherepanov. High Temp., **59**(3), 198(2021). DOI: 10.1134/S0018151X21030019.